ACS APPLIED MATERIALS & INTERFACES

Research Article

www.acsami.org

Blood Compatibility Evaluations of Fluorescent Carbon Dots

Sha Li, Zhong Guo, Yi Zhang, Wei Xue, and Zonghua Liu*

Key Laboratory of Biomaterials of Guangdong Higher Education Institutes, Department of Biomedical Engineering, Jinan University, Guangzhou, 510632, China

Supporting Information

ABSTRACT: Because of their unique advantages, fluorescent carbon dots are gaining popularity in various biomedical applications. For these applications, good biosafety is a prerequisite for their use in vivo. Studies have reported the preliminary biocompatibility evaluations of fluorescent carbon dots (mainly cytotoxicity); however, to date, little information is available about their hemocompatibility, which could impede their development from laboratory to bedside. In this work, we evaluated the hemocompatibility of fluorescent carbon dots, which we prepared by hydrothermal carbonization of α-cyclodextrin. The effects of the carbon dots on the structure and function of key blood components were investigated at cellular and molecular levels. In particular, we considered the morphology and lysis of human red blood cells, the structure and conformation of the plasma protein fibrinogen, the complement activation, platelet activation, and in vitro and in vivo blood coagulation. We found that the carbon dots have obvious concentration-dependent effects on the blood components. Overall, concentrations of the fluorescent carbon dots at ≤0.1 mg/mL had few adverse effects on the blood components, but at higher doses, the carbon dots impair the structure and function of the blood components, causing morphological disruptions and lysis of red blood cells, interference in the local microenvironments of fibrinogen, activation of the complement system, and disturbances in the plasma and whole blood coagulation function in vitro. However, the carbon dots tend to activate platelets only at low concentrations. Intravenous administration of the carbon dots at doses up to 50 mg/kg did not impair the blood coagulation function. These results provide valuable information for the clinical application of fluorescent carbon dots.

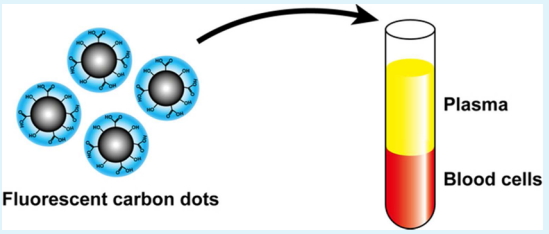

KEYWORDS: *fluorescent carbon dots, hemocompatibility, blood compatibility, biocompatibility, red blood cells, blood coagulation*

1. INTRODUCTION

Fluorescent carbon dots are a type of novel nanomaterial (generally, the diameter <10 nm) with a photoluminescent behavior.[1] Since their discovery in 2004,[2] the preparation of fluorescent carbon dots and their applications have expanded rapidly, with new types constantly emerging.[3,4] Compared to other fluorescent nanomaterials, fluorescent carbon dots have various advantages, such as typical size and/or excitation wavelength-dependent photoluminescence, photostability, easy surface functionalization, low toxicity, and diverse preparation methods.[3,4] Fluorescent carbon dots have attracted much attention for many biomedical applications including biological probes, bioimaging, cell labeling, biosensors, disease diagnosis, drug delivery, etc.[3,4]

In biomedical applications, fluorescent carbon dots are usually introduced in vivo by various routes and good biocompatibility is mandatory for their safe application. Previously, different researchers have evaluated the in vitro cytotoxicity of fluorescent carbon dots.[5] Dhara et al. studied the in vitro blood compatibility of fluorescent carbon dots by measuring hemolysis and observing the aggregation of red blood cells (RBCs), white blood cells, and platelets.[5] In addition, Sun et al. reported the in vivo distribution, clearance, and toxicity of fluorescent carbon dots.[6] Despite these reports and the exponential increase in the types of fluorescent carbon dots, their biosafety is still not clearly understood. In particular, information about their blood compatibility is lacking, which is hindering the biomedical development from the lab to the clinic.

In many clinical applications, fluorescent carbon dots administered in vivo unavoidably contact blood tissue and interact with various blood components. The interactions can affect the metabolism of blood tissue, and inevitably, the whole organism, and even the in vivo fate of the fluorescent carbon dots themselves. Hence, the fluorescent carbon dot-blood interaction needs to be clearly elucidated. In this work, we first synthesize fluorescent carbon dots by the hydrothermal carbonization of α-cyclodextrin. We then investigate the effects of the fluorescent carbon dots on the structure and function of key blood components; specifically, the morphology and lysis of human RBCs, structural and conformational changes of the plasma protein fibrinogen, the complement activation, platelet activation, and in vitro and in vivo blood coagulation. We provide significant information on the blood compatibility of fluorescent carbon dots, to help direct their design and clinical applications.

Received: June 3, 2015
Accepted: August 13, 2015
Published: August 13, 2015

DOI: 10.1021/acsami.5b04866
ACS Appl. Mater. Interfaces 2015, 7, 19153−19162

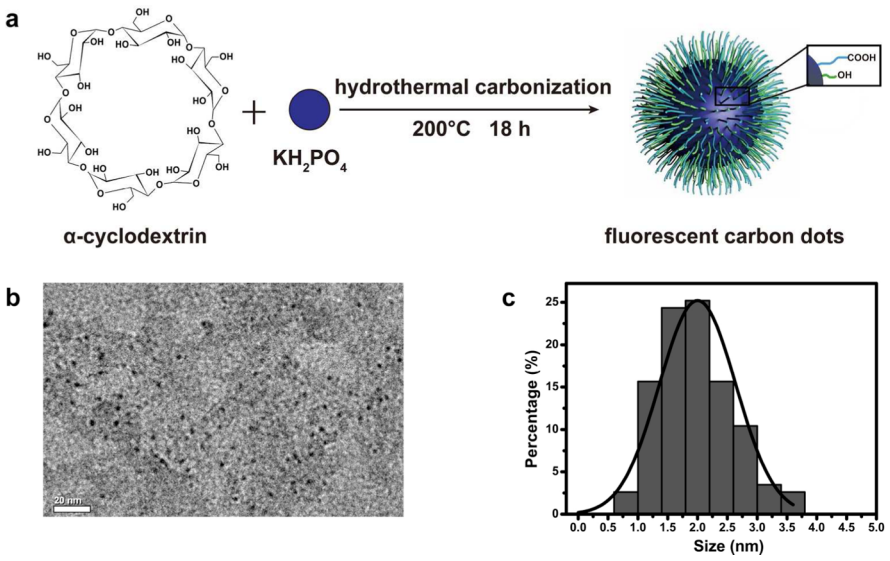

Figure 1. Synthesis of the fluorescent carbon dots and their size. (a) Schematic illustration of the synthesis procedure of the fluorescent carbon dots. (b) HRTEM image of the fluorescent carbon dots. (c) Corresponding diameter distribution histogram of the fluorescent carbon dots, measured by ImageJ 1.47 v.

2. MATERIALS AND METHODS

2.1. Materials. α-Cyclodextrin (purity ≥98%) and fibrinogen were purchased from Sigma-Aldrich (USA). KH_2PO_4 (≥99.5%) was purchased from Guangzhou Chemical Reagent Factory (Guangzhou, China). Quinine sulfate dehydrate (purity ≥98%) was purchased from Aladdin (Shanghai, China). Fresh blood from healthy, consenting volunteers was collected in sodium citrate tubes with a blood/anticoagulant ratio of 9:1.

2.2. Preparation of Fluorescent Carbon Dots. α-Cyclodextrin (0.43 g) and KH_2PO_4 (1.09 g) were dissolved in 40 mL of deionized water, and transferred into a poly(tetrafluoroethylene) autoclave (100 mL), and then subjected to ultrasonic treatment for 20 min at room temperature. Then, N_2 was blown into the solution for 1 h to exclude O_2 from the reaction system. The autoclave was put into an oven and heated at 200 °C for 18 h. After the mixture was cooled, the resulting black precipitates were removed by centrifugation at 7000 rpm for 10 min. The yellow supernatant was collected and freeze-dried. The white floccule thus obtained was dissolved in anhydrous ethanol. The solution was centrifuged and the resulting yellow supernatant was collected, filtered through 0.2 μm filters, and rotary evaporated to obtain the fluorescent carbon dots. The preparation procedure for the fluorescent carbon dots is illustrated in Figure 1.

2.3. Characterization of the Fluorescent Carbon Dots. *2.3.1. Physiochemical Characterizations of the Fluorescent Carbon Dots.* The morphology of the fluorescent carbon dots was observed by a high-resolution transmission electron microscope (HRTEM, JEOL-2100F, Japan). The sample for the HRTEM was prepared by dropping the fluorescent carbon dot aqueous solution onto a copper grid and air drying for 1 h at room temperature. The mean hydrodynamic size and zeta potential of the fluorescent carbon dots, dissolved in Milli-Q-purified water (100 μg/mL), was measured with a zeta potential analyzer (Zetasizer Nano ZS, Malvern Instruments Ltd., UK). The chemical structures of the fluorescent carbon dots and α-cyclodextrin were characterized by Fourier transformed infrared spectrophotometer (FTIR) (BRUKE, VERTEX 70, Germany) with the potassium bromide (KBr) pellet technique. The UV−visible absorption spectrum of the fluorescent carbon dot aqueous solution was recorded using a UV-2550 spectrophotometer (Shimadzu Corporation, Japan). The fluorescence emission spectra of the fluorescent carbon dot aqueous solution were recorded on a Hitachi F-7000 fluorescence spectrophotometer (Hitachi High-Technologies Corp., Tokyo, Japan). The UV−visible absorption and fluorescence emission spectra measurements were performed in 1 cm quartz cuvettes at room temperature.

2.3.2. Quantum yield measurement. Quantum yield is an important parameter for evaluating the fluorescence strength of fluorescence carbon dots. It is calculated with the equation[1]

$$\Phi = \Phi_R \times \frac{I}{I_R} \times \frac{A_R}{A} \times \frac{\eta^2}{\eta_R{}^2}$$

where Φ is the quantum yield, I is the integrated fluorescence intensity, A is the absorbance intensity, and η is the refractive index. The quinine sulfate (Φ = 0.54) in 0.1 M H_2SO_4 is used as a reference fluorophore. In this equation, the subscript R refers to the reference. The quantum yield of the fluorescent carbon dot aqueous solution was measured at an excitation wavelength of 350 nm.

2.3.3. Cell Imaging. The HeLa cells (4×10^4 cells/mL) were seeded on sterile WHB coverslips (WHB, China), on the bottom of 24-well plates, and cultured (37 °C, 5% CO_2) overnight. After the cells adhered to the coverslips, the cells were treated with the fluorescent carbon dots dissolved in fetal bovine serum-free Dulbecco's modified Eagle medium. The cells were then washed three-times with fresh phosphate buffered saline (PBS, pH7.4), and fixed with 4% formaldehyde for 10 min at room temperature. After they were washed with the PBS, the cells were mounted with glycerol and then observed with a confocal laser scanning microscope (LSM 700, Zeiss, Germany).

2.4. Effect of Fluorescent Carbon Dots on RBC Morphology and Lysis. *2.4.1. RBC Morphology.* Fresh whole blood was centrifuged at 1000 × g for 5 min, and the supernatant was carefully removed. The RBC pellet was washed with PBS, and then incubated for 10 min at room temperature with different concentrations of the fluorescent carbon dot solution, dissolved in PBS. After that, the RBCs were fixed for 2 h with 4% formaldehyde, and subjected to a dehydration gradient with ethanol solutions (75, 85, 95, and 100%, v/v). After air drying, the RBCs were coated with gold and observed with a scanning electron microscope (SEM, Philips XL-30, Holland).

2.4.2. RBC Lysis. Fifty mL of RBC suspension (16% in PBS, v/v) was added to 1 mL of PBS (as a negative control) or different concentrations of the fluorescent carbon dot solutions dissolved in PBS. As a positive control, 50 μL of the RBC suspension was added to 1 mL of water to yield complete hemolysis. After incubation for a certain time, the RBC suspensions were centrifuged at 1000 × g for 5 min, and the supernatants were collected. Then, the absorbance values of the released hemoglobin (Hb) in the supernatants (200 μL) were measured at 540 nm with a microplate reader (Multiskan MK3; Thermo Lab-systems, Finland). The hemolysis in the presence of the

DOI: 10.1021/acsami.5b04866
ACS Appl. Mater. Interfaces 2015, 7, 19153−19162

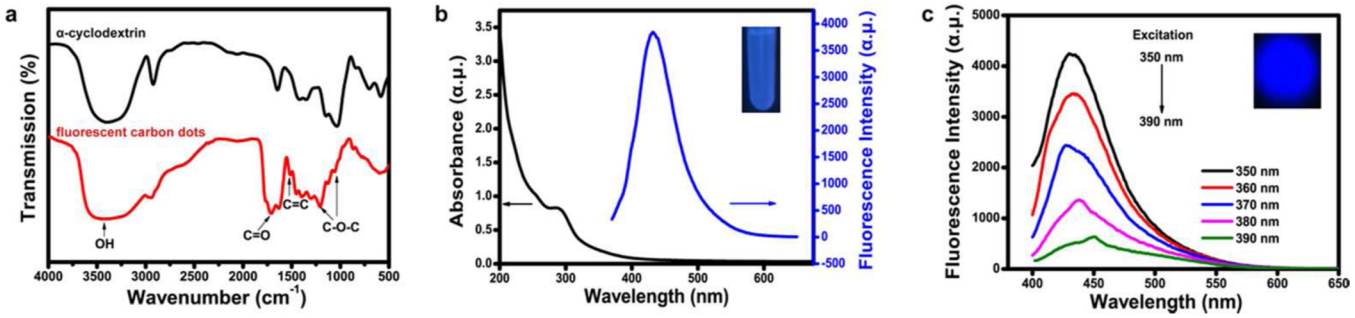

Figure 2. Spectra of the fluorescent carbon dots. (a) FTIR spectra of α-cyclodextrin and the fluorescent carbon dots. (b) UV−visible absorption spectrum (black line) and fluorescence emission spectrum (blue line) of the fluorescent carbon dots excited at 350 nm. Inset: Photograph of the fluorescent carbon dots aqueous solution under UV light at 365 nm. (c) Fluorescence emission spectra of the fluorescent carbon dots at a series of excitation wavelength from 350 to 390 nm. Inset: Fluorescence microscopy image of the aqueous solution of the fluorescent carbon dots excited at 365 nm.

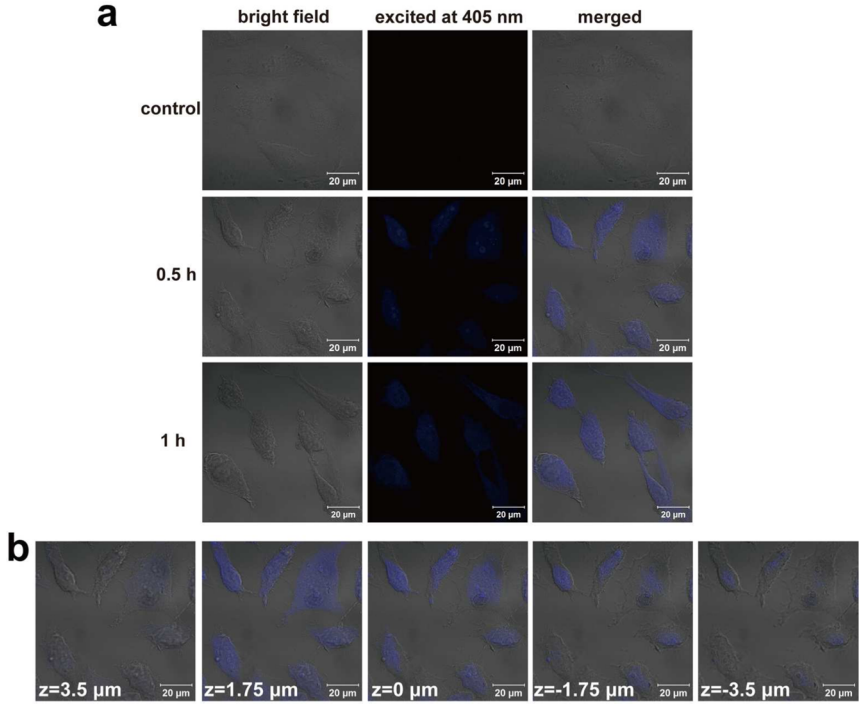

Figure 3. Hela cells incubated with the fluorescent carbon dots as observed with a confocal laser scanning microscope. (a) Hela cells incubated with the fluorescent carbon dots at 37 °C for 0.5 or 1 h. (b) *z*-axis scanning image of the Hela cells incubated with the fluorescent carbon dots for 0.5 h.

fluorescent carbon dots was calculated by comparing the absorbance values of the tested supernatants to that of the positive control (i.e., 100% hemolysis).

2.5. Effect of Fluorescent Carbon Dots on Fibrinogen Structure and Conformation. *2.5.1. Fluorescence Spectroscopy.* The fluorescence spectra of fibrinogen (0.5 mg/mL) in the absence or presence of the fluorescent carbon dots were recorded at λ_{exc} = 280 nm on a Hitachi F-7000 fluorescence spectrophotometer (Hitachi High-Technologies Corp, Tokyo, Japan). All of the fluorescence emission spectra were obtained by subtracting the values for the corresponding concentrations of the fluorescent carbon dot solutions in PBS. The measurement parameters for all fluorescence spectra were: voltage at 500 V, scan rate at 1200 nm/min, slit width of 5 nm, and λ_{em} from 300 to 650 nm.

2.5.2. Circular Dichroism Spectroscopy. The circular dichroism spectra of fibrinogen (0.5 mg/mL) in the absence or presence of the fluorescent carbon dots were recorded at 25 °C in a nitrogen atmosphere in a 5 mm cuvette by using an Applied Photophysics Chirascan CD spectrometer (Applied Photophysics Ltd., Leatherhead, U.K.). PBS was used as the running buffer. All of the circular dichroism spectra were obtained with three scans recorded from 190 to 260 nm at a scan rate of 60 nm/min, and finally presented as the average molar ellipticity (θ) after deducting the values for the corresponding concentrations of the carbon dot solutions in PBS.

2.6. Complement Activation by Fluorescent Carbon Dots. To evaluate the complement activation elicited by the fluorescent carbon dots, the cleavage of complement component C3 was detected by measuring its activation peptides (C3a) with a commercial C3a enzyme immunoassay kit (eBioscience Inc., San Diego, USA).[7] Briefly, fresh anticoagulated whole blood was centrifuged at 1000 × *g* for 10 min, and the resulting supernatant (platelet-poor plasma) was collected. The platelet-poor plasma was mixed at a volume ratio of 1:1 with different concentrations of the fluorescent carbon dot solutions in PBS, and incubated at 37 °C for 30 min. Then, the plasma-fluorescent carbon dots mixture was diluted (×1000) with a dilution buffer provided in the kit. The diluted samples (100 μL) were added to a microwell plate provided in the kit, which was precoated with an antihuman C3a antibody. The diluted samples in the wells were incubated for 1 h at 25 °C to allow the C3a present in the samples to bind to the coated antibody. Unbound components were

DOI: 10.1021/acsami.5b04866
ACS Appl. Mater. Interfaces 2015, 7, 19153−19162

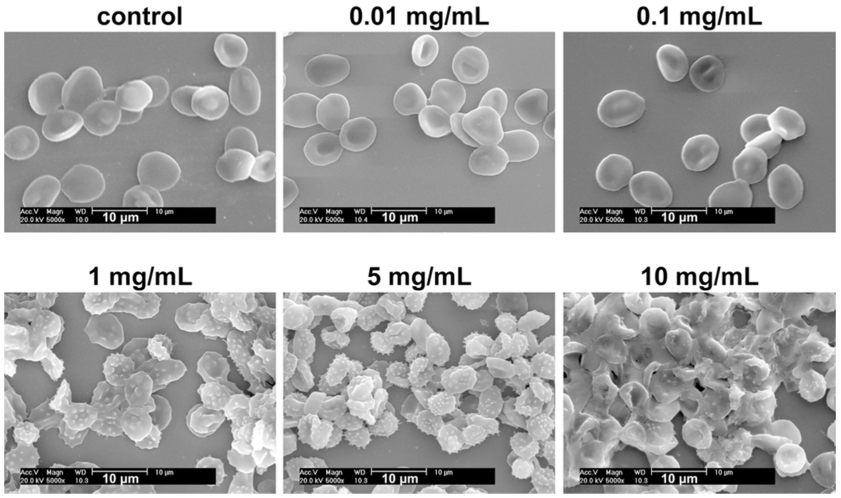

Figure 4. Morphology and aggregation of the RBCs in the presence of different concentrations of the fluorescent carbon dots as observed with SEM.

removed by washing. A biotin-conjugated antihuman C3a antibody was added to the wells, incubated at 25 °C for 2 h, and removed by washing. A streptavidin-horseradish peroxidase was added to the wells, incubated at 25 °C for 2 h, and removed by washing. A substrate solution was added to the wells, and incubated at 25 °C for 30 min. After adding a colored product, the absorbance of the solutions in the wells was measured at 450 nm with the microplate reader (Multiskan MK3; Thermo Lab-systems, Finland). PBS and inulin solution (10 mg/mL in PBS) were used as a negative and positive control, respectively. C3a concentrations in the samples were calculated by using a standard curve.

2.7. Effect of Fluorescent Carbon Dots on in Vitro Blood Coagulation. *2.7.1. Activated Partial Thromboplastin Time (APTT) and Prothrombin Time (PT).* Fresh, anticoagulated whole blood was centrifuged at 1000 × *g* for 10 min, and the resulting supernatant (platelet-poor plasma) was collected. The platelet-poor plasma (270 μL) was mixed with the fluorescent carbon dot solutions (30 μL in PBS). After adding corresponding reagents, the APTT and PT of the samples were measured with an automatic coagulation analyzer (STAR evolution, Diagnostica Stago, France).

2.7.2. Thromboelastography (TEG). Fresh citrate whole blood was mixed at a volume ratio of 9:1 with different concentrations of the fluorescent carbon dot solutions (in PBS) in kaolin-containing tubes. Then, 20 μL of $CaCl_2$ solution (0.2 M) and 340 μL of the fluorescent carbon dots/blood mixture were sequentially added to a TEG cup. The coagulation process was recorded at 37 °C using a Thromboelastograph Hemostasis System 5000 (Hemoscope Corporation, Niles, IL, USA).

2.8. Platelet Activation by Fluorescent Carbon Dots. Fresh citrate-anticoagulated whole blood was centrifuged at 100 × *g* for 5 min, and the supernatant platelet-rich plasma was collected and diluted with PBS at a volume ratio of 1:1. The resulting platelet suspension (90 μL) was incubated for 30 min with 10 μL of the solutions of fluorescent carbon dots in PBS. Ten microliters of the fluorescent carbon dots/platelet mixture was diluted in 90 μL of *N*-(2-hydroxyethyl)piperazine-*N*′-(2-ethanesulfonic acid) (HEPES) buffer, and then incubated in the dark for 10 min with 5 μL of anti-CD62P-PE and 5 μL of anti-CD42b-FITC (both from eBioscience Inc., San Diego, USA). The expression of platelet activation marker CD62P (P-Selectin) was measured using a flow cytometer (Calibur, BD Biosciences, USA). Bovine thrombin (1 U/mL) was used to activate the platelets as a positive control. Mouse IgG-PE was used as a nonspecific binding control.

2.9. Effect of Intravenously Administered Fluorescent Carbon Dots on Blood Coagulation. Twenty Wistar rats (200 ± 20 g) were randomly divided into four groups (five each). The rats were intravenously injected via the tail vein with solutions of the carbon dots dissolved in saline. The injected doses for each group were normalized to be 0.5, 5, or 50 mg/kg per rat, and saline was used as the control. At 24 h, the rats were anesthetized, and the whole blood was collected into citrate tubes for APTT and PT assays.

2.10. Statistical Analysis. The data was represented as the mean ± SD (standard deviation) and statistically analyzed using a one-way ANOVA with SPSS 16.0. The difference was considered significant when $p < 0.05$ (*) and $p < 0.01$ (**).

3. RESULTS AND DISCUSSION

3.1. Physicochemical Characterization of Fluorescent Carbon Dots. In this work, a carbon source α-cyclodextrin was used to prepare the fluorescent carbon dots by referring to a simple and green hydrothermal carbonization method[1] (Figure 1a). The resulting fluorescent carbon dots were highly water-soluble. According to HRTEM observations (Figure 1b), the fluorescent carbon dots were fairly monodisperse, uniform, spherical nanoparticles with diameters <10 nm (Figure 1c). FTIR spectroscopy was used to identify the functional groups on the surface of the fluorescent carbon dots. In the FTIR spectrum of the fluorescent carbon dots (Figure 2a), the peaks at 1707 and 1624 cm^{-1} corresponded to the C═O stretching vibration in amide and carbonyl bonds.[8] The characteristic peak at 1516 cm^{-1} was assigned to the stretching of C═C.[8] The

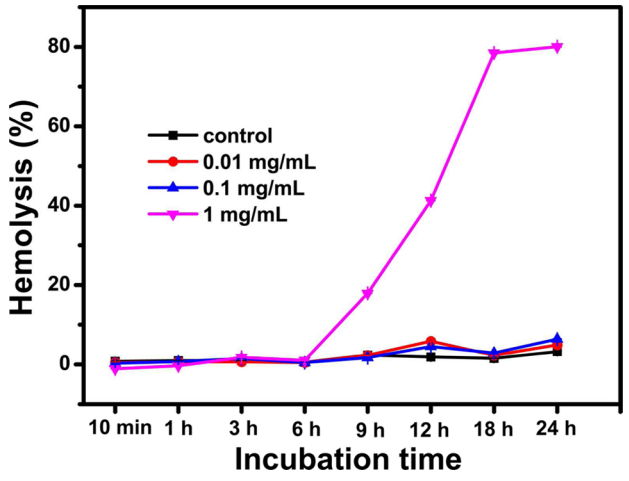

Figure 5. Hemolysis of the RBCs incubated with different concentrations of the fluorescent carbon dots at room temperature.

DOI: 10.1021/acsami.5b04866
ACS Appl. Mater. Interfaces 2015, 7, 19153−19162

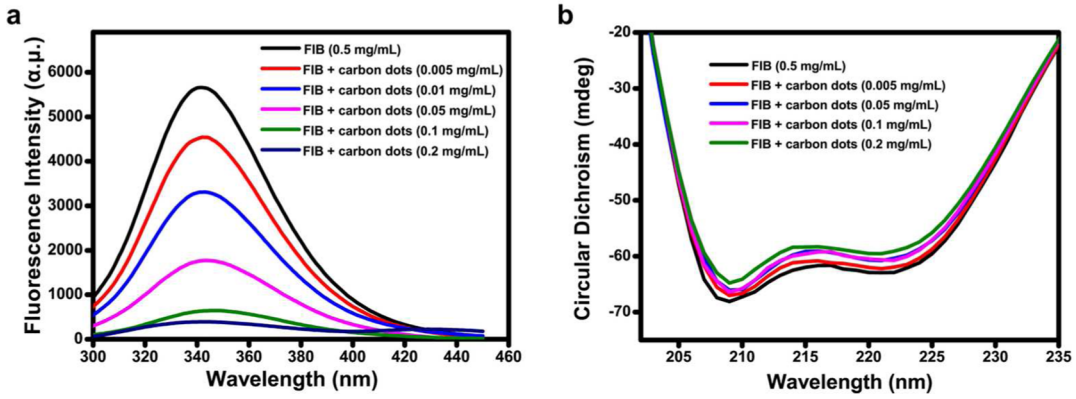

Figure 6. Fluorescence spectra (a) and CD spectra (b) of fibrinogen (FIB) in the absence and presence of the fluorescent carbon dots.

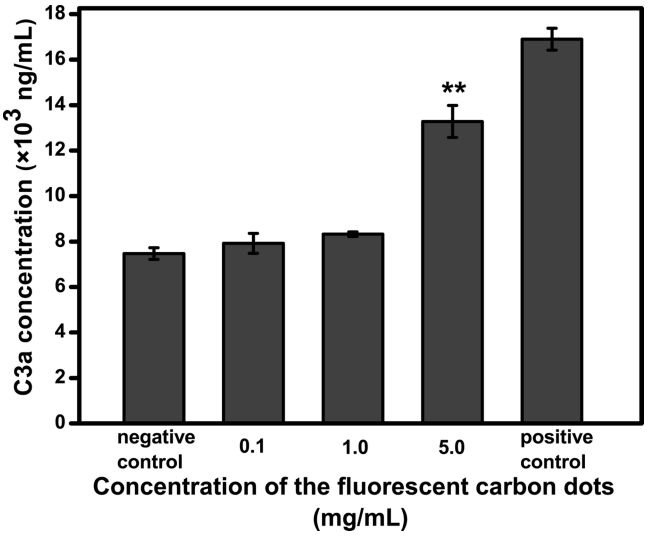

Figure 7. Complement activation in vitro by the fluorescent carbon dots with PBS as a negative control and inulin (10 mg/mL) as a positive control.

broad band at 3388 cm^{-1} was associated with O−H bonds. The peaks at 1055 and 1125 cm^{-1} corresponded to the stretching vibration of the C−O−C groups.[1] The peaks suggest that abundant functional groups (such as hydroxyl and carboxyl groups) were present on the surface of the fluorescent carbon dots.[4] These groups could introduce different defects on the surface of the fluorescent carbon dots, acting as excitation energy traps and leading to different optical properties.[4] Also, the fluorescent carbon dots had excellent water solubility because of these groups. Moreover, the existence of the carboxyl groups led to the negative surface of the fluorescent carbon dots, as confirmed by the zeta potential of the fluorescent carbon dots (measured as −6.32 ± 1.27 mV).

Figure 2b shows the UV−visible absorption and fluorescence emission spectra of the fluorescent carbon dots. The UV−visible absorption spectrum showed a peak at around 287 nm, which is attributable to the $\pi-\pi^*$ transition of aromatic sp^2 domains.[9] A strong fluorescence emission peak at 430 nm was observed when the fluorescent carbon dots were excited at 350 nm. The insert in Figure 2b shows the optical image of the fluorescent carbon dots under UV lamp (λ = 365 nm), from which a bright blue fluorescence could be seen by the naked eye. The fluorescent carbon dots also displayed the characteristic excitation-dependent emission (Figure 2c). When the excitation wavelength was increased from 350 to 390 nm, the fluorescence emission intensity decreased, and the maximum emission peak position shifted to a longer wavelength. The red shift could be attributed to the different size of fluorescent carbon dots.[1] The insert in Figure 2c shows the blue fluorescence microscopy image of the fluorescent carbon dots excited at 365 nm. In addition, the fluorescence quantum yield

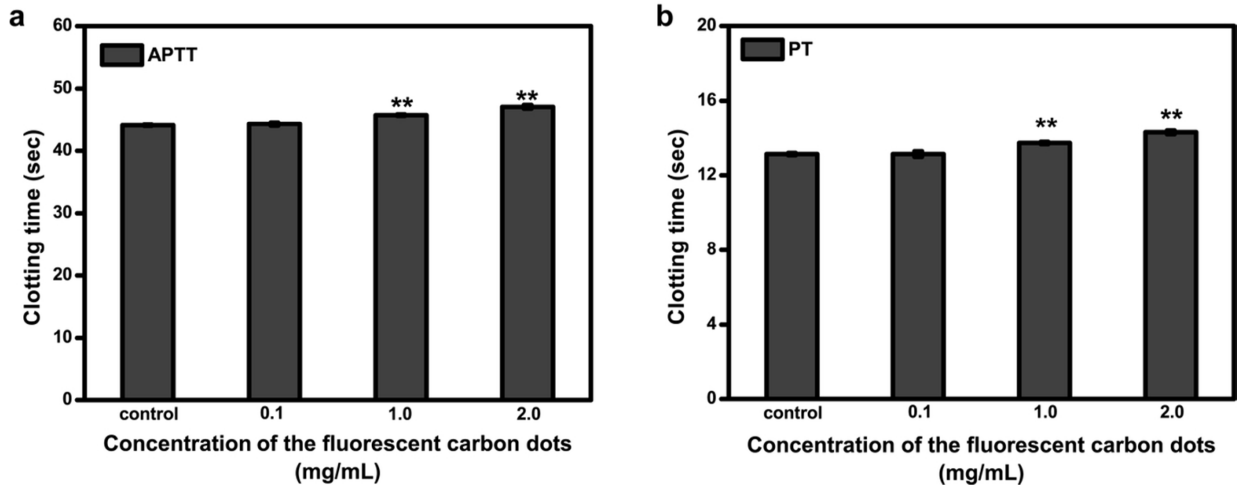

Figure 8. APTT (a) and PT (b) of in vitro plasma coagulation in the presence of the fluorescent carbon dots with PBS as a negative control.

DOI: 10.1021/acsami.5b04866
ACS Appl. Mater. Interfaces 2015, 7, 19153−19162

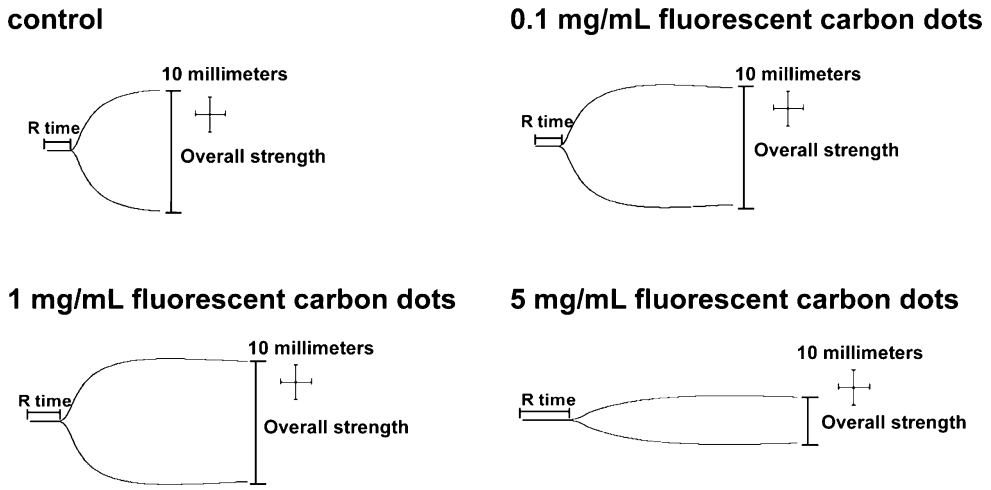

Figure 9. TEG traces of in vitro whole blood coagulation in the presence of the fluorescent carbon dots with PBS as a control.

Table 1. Clotting Kinetics Values of Human Whole Blood Containing the Fluorescent Carbon Dots[a]

samples	*R* (min)	*K* (min)	*α* (deg)	MA (mm)
normal range	5−10	1−3	53−72	50−70
PBS control	6.7	2.5	57.1	51.0
0.1 mg/mL carbon dots	6.8	2.8	53.5	51.5
1 mg/mL carbon dots	8.2	2.7	52.4↓	53.1
5 mg/mL carbon dots	13.4↑	N/A	19.2↓	18.9↓

[a]The sign ↓ indicates a low value, and ↑ indicated a high value compared with the normal range provided by the TEG analyzer.

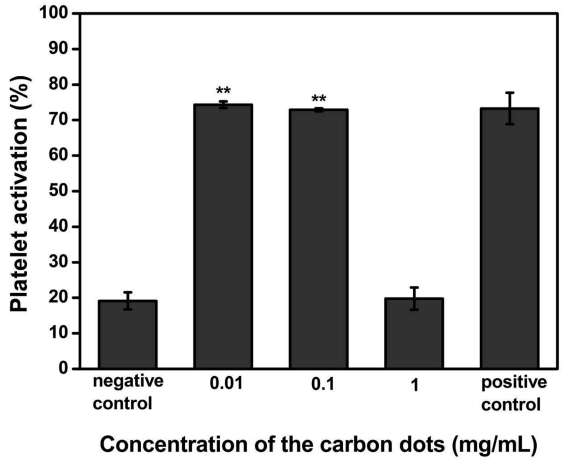

Figure 10. Platelet activation in vitro by the fluorescent carbon dots.

of the fluorescent carbon dots, the ratio of photons absorbed to photons emitted through fluorescence, was also measured against the quinine sulfate reference sample (λ_{exc} = 350 nm). By calculation, the fluorescence quantum yield of the fluorescent carbon dots was 2.16%.

3.2. Cell Image. Many researchers have reported that fluorescent carbon dots are promising imaging agents because of their strong fluorescent property and excellent biocompatibility. In this study, HeLa cells were cocultured with the fluorescent carbon dots in vitro (100 μg/mL dissolved in DMEM), and the internalized fluorescent carbon dots were observed. Figure 3a shows that the intracellular fluorescent carbon dots could emit a bright blue fluorescence under an excitation wavelength of 405 nm. In addition, the fluorescence intensity at 30 min was as bright as that at 1 h, demonstrating that the fluorescent carbon dots were quickly taken up by the cells. The uptake of the fluorescent carbon dots was further verified by *Z*-axis scanning confocal microscopy (Figure 3b). Further, the cellular uptake of the carbon dots by Hela cells was quantitatively analyzed using flow cytometry (see Supporting Information and Figure S1). After 1 h of incubation, the cellular uptake percentage reached almost 100% in the presence of 0.5 or 1 mg/mL of the carbon dots, while 0.1 mg/mL of the carbon dots resulted in a cellular uptake of only 6.53%. Thus, the cellular uptake percentage appears to depend on the concentration of the carbon dots. The above results suggest that the fluorescent carbon dots used in this work have characteristics in common with the fluorescent carbon dots reported in the literatures.

3.3. Effect of Fluorescent Carbon Dots on RBC Morphology and Lysis. *3.3.1. RBC Morphology.* RBCs have been widely used in biosafety evaluations of various biomedical materials. Being responsible for the transport of oxygen and carbon dioxide, RBCs are the most abundant blood cells, making up 40−50% (v/v) of human whole blood. In most cases, blood-contact biomaterials will inevitably interact with RBCs. Moreover, because of their high abundance and easy handling, RBCs are a good model for preliminary investigations of the complicated interactions between other mammalian cell membranes and foreign biomaterials. In this work, we studied the effect of fluorescent carbon dots on the morphology and lysis of RBCs to determine the interaction of the carbon dots with RBC membrane structure.

Normal, mature RBCs display the shape of biconcave disks. They are very sensitive to membrane-active substances that interact with the RBC membrane and alter the morphology of the RBCs. Figure 4 shows RBCs in the presence of different concentrations of the fluorescent carbon dots. Overall, the carbon dots appear to affect the RBC morphology in a concentration-dependent manner. Specifically, the morphology of the RBCs in 0.01 and 0.1 mg/mL of the carbon dots did not change, compared with the control. Nevertheless, the RBCs became crenated in 1 mg/mL of the carbon dots. Pointed spicules spread on the RBCs in 5 mg/mL of the carbon dots. The RBCs in 10 mg/mL of the carbon dots were broken and aggregated together. The results show that the carbon dots had a strong interaction with the RBC membrane.

DOI: 10.1021/acsami.5b04866
ACS Appl. Mater. Interfaces 2015, 7, 19153−19162

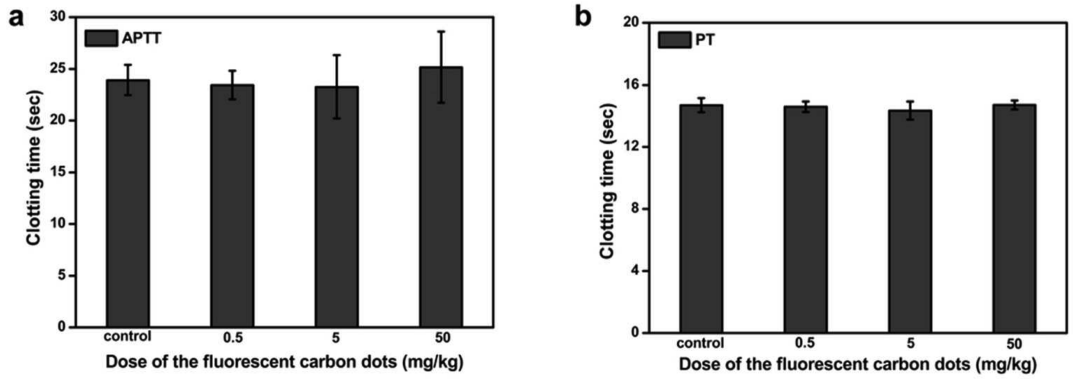

Figure 11. Effect of the intravenously administered fluorescent carbon dots on APTT and PT.

Biomaterial-RBC interactions have been reported to be mediated by electrostatic attraction between the positively charged biomaterials; the negative RBC surface and hydrophobic interactions between the hydrophobic structures of biomaterials and the RBC lipid layer; H bonds; and van der Waals' force, etc.[10] An electrostatic attraction between the carbon dots and the RBC surface seems impossible in view of the negative zeta potential of the carbon dots, as mentioned above. Instead, hydrophobic interaction forces are more likely mediating the interaction between the carbon dots and the RBC surface. On one hand, the effect of carbon dots on RBC morphology is similar to that of hydrophobically modified polymers, which changes RBCs from normally biconcave to crenated, in a concentration-dependent way.[11,12] On the other hand, hydrophobic aromatic ring structures have been proposed to exist in the inner core of the fluorescent carbon dots, synthesized by the hydrothermal carbonization of saccharides.[13,14] The carbon dots could be adsorbed to the RBC surface by means of the hydrophobic interaction of their hydrophobic structures with the RBC lipid bilayer, further affecting the morphology and integrity of the RBC membrane structure. In contrast, adsorption of carbon dots to nucleated tissue cells could induce rapid internalization of the carbon dots into the cells, as demonstrated above.

3.3.2. RBC Lysis. Hemolysis refers to the release of hemoglobin from RBCs, and indicates the disturbance of RBC membrane integrity. Like RBC morphology, hemolysis also reflects the interaction of biomaterials with the RBC membrane. Hemolysis has been widely used in the biosafety evaluations of various biomedical materials. In this work, Figure 5 shows the hemolysis percentage of RBCs exposed to different concentrations of the fluorescent carbon dots along with incubation times, up to 24 h. From the figure, RBCs in 0.01 and 0.1 mg/mL of the carbon dots did not lyse even at an incubation time of 24 h, compared to the PBS control. Nevertheless, the RBCs in 1 mg/mL of the carbon dots started to lyse from 6 h, reaching 85% at 24 h. The results indicate that RBC lysis in the presence of carbon dots was dose- and time-dependent. The hemolysis increased with increasing concentrations of carbon dots and incubation time, suggesting that the RBC membrane disturbance caused by the carbon dots was a continuous process. Combining this result with RBC morphology, we speculate that the carbon dots are adsorbed to the RBC membrane in a concentration-dependent way, and that the adsorbed carbon dots on the RBC membrane disturb the RBC membrane structure and integrity. Nevertheless, it could also be inferred that the effect of the carbon dots on membrane structure of normal nucleated cells could be alleviated through their internalization into the cells.

3.3.3. Interaction of Carbon Dots with RBCs in the Presence of Albumin. We further observed the morphology of carbon dot-treated RBCs in the presence of bovine serum albumin (BSA), to elucidate the molecular interaction between the carbon dots, RBCs, and plasma proteins. To this aim, RBCs were treated with 10 mg/mL of the carbon dots and then washed twice with 20 mg/mL BSA. From SEM observations (Figure S2), the washing with BSA restored the carbon dot-treated RBC morphology to their normal biconcave disk shape. Since plasma protein albumin is known not to adsorb to RBCs,[11] it could not directly repair the distorted morphology of the RBCs caused by the carbon dots. The BSA molecules likely interacted with the carbon dots, detached them from the RBC surface, and alleviated the RBC membrane disturbance. In addition, we tested the lysis of carbon dot-treated RBCs in the presence of BSA (Supporting Information, Figure S3). The lysis of carbon dot-treated RBCs was greatly attenuated in the presence of 5 mg/mL BSA, suggesting that the presence of BSA suppressed the disturbance of the RBC membrane caused by the carbon dots. This further confirms that the interaction of carbon dots with BSA detached part of the carbon dots from the RBC membrane.

From the above results, we speculate on the molecular interaction of carbon dots with RBCs and plasma proteins. First, the carbon dots adsorbed to the RBC surface through physical interaction forces, which is a reversible process. Electrostatic attraction between BSA and the carbon dots seems improbable since both are negatively charged. As we previously reported, hydrophobically modified polymers can adsorb to the RBC surface by intercalating with the lipid bilayer of the RBC membrane, leading to the formation of echinocytes and hemolysis.[11] Similarly, hydrophobic interaction can be the main force mediating the adsorption of carbon dots to the RBC membrane, as found in this work, due to the presence of hydrophobic structures in the carbon dots.[13,14] In addition, we found that serum albumin can detach the hydrophobically modified polymers from the RBC surface via hydrophobic interactions with the polymers.[11] The BSA molecule has a hydrophobic cavity for carrying some cargos, such as lipid-soluble hormones, free fatty acids, and hydrophobic drugs.[11] Similarly, BSA may interact with the carbon dots via hydrophobic interactions, detaching the carbon dots from the RBC surface, and alleviating the membrane disturbance in morphology and integrity. Taken together, these results demonstrate that the negatively charged carbon dots with

DOI: 10.1021/acsami.5b04866
ACS Appl. Mater. Interfaces 2015, 7, 19153−19162

their hydrophobic structures interact with the RBCs or serum albumin (the most abundant plasma protein) mainly through hydrophobic interactions.

3.4. Effect of Fluorescent Carbon Dots on Fibrinogen Structure and Conformation. Fluorescent carbon dots are typically administered directly into the bloodstream in biomedical applications, such as bioimaging. Once in contact with blood tissue, the carbon dots are immediately covered by the abundant plasma proteins, leading to the formation of a protein "corona" on their surfaces.[15] The complex interaction between the fluorescent carbon dots and the plasma proteins can cause adverse effects, such as alterations to the structure and conformation of plasma proteins and deficiencies in their normal biofunctions, in turn, causing blood tissue dysfunction. Therefore, the effect of fluorescent carbon dots on plasma proteins must be elucidated to promote scientific designs for safe clinical applications.

We studied the effect of carbon dots on the structure and conformation of fibrinogen, which is a highly abundant plasma glycoprotein and a key component of the blood coagulation system. Fibrinogen is converted into water-insoluble fibrin by activated thrombin to form three-dimensional blood coagula with activated platelets. The proper structure and conformation of fibrinogen is important for maintaining normal biofunctions in the blood coagulation process. Structural and conformational changes of fibrinogen can be detected at the molecular level using spectroscopic methods like fluorescence emission and CD spectroscopies.

3.4.1. Fluorescence Spectroscopy. Fluorescence spectroscopy has often been used to examine the effect of biomaterials or drugs on the structure and conformation of proteins. The tryptophan residue is the most important fluorophore (intrinsic fluorescence emission) in proteins with its fluorescence peak (λ_{max}) around 341 nm. Tryptophan residues are mainly located inside the hydrophobic cores of proteins, and are highly sensitive to their local hydrophobic environment. With structural changes in proteins, tryptophan residues can be exposed to the surrounding polar solvent, leading to the intensity attenuation and/or position shift of the fluorescence emission peak. Therefore, the fluorescence spectral alteration of proteins can be used to indicate their structural and conformational alterations in the presence of biomaterials or drugs.

Figure 6a shows the fluorescence spectra of fibrinogen in the absence and presence of the fluorescent carbon dots. The fluorescence peaks at 342 nm decreased in intensity but did not shift with the increasing concentration of carbon dots. The fluorescence emission intensity of fibrinogen, excited at 280 nm, is usually dominated by tryptophan residues. The result indicates that the carbon dots caused fluorescence quenching of fibrinogen because of the changed microenvironments around the tryptophan residues (i.e., from hydrophobic to hydrophilic). This implies that the carbon dots interacted with fibrinogen, altering the local microenvironments around the tryptophan residues.

3.4.2. CD Spectroscopy. CD spectroscopy is an excellent tool for studying the secondary structures (α-helices, β-sheets, and turns) of proteins. To further understand the effect of carbon dots on fibrinogen structure and conformation, the CD spectra of fibrinogen were obtained in the absence or presence of the carbon dots (Figure 6b). The negative peaks at 208 and 222 nm in the CD spectrum of pure fibrinogen were typical characteristics of the α-helix of the protein. The ellipticity at 208 and 222 nm slightly decreased in the presence of carbon dots, indicating their weak effect on the α-helix structure of fibrinogen.

Collectively, we conclude that the carbon dots obviously disturbed the local microenvironments of fibrinogen, but only weakly affected its secondary structure α-helix. Protein adsorption to various biomaterials has been reported to be mediated by hydrophobic interactions, electrostatic attraction, H bonds, and/or van der Waals' force, etc.[15] Among these, hydrophobic interaction is considered as the primary mediator of fibrinogen/biomaterial interaction.[16] Here, we hypothesize that hydrophobic interaction could be the main force mediating the interaction between the carbon dots and fibrinogen.

3.5. Complement Activation by Fluorescent Carbon Dots. The complement system in humans consists of about 35−40 proteins free in the blood plasma or attached to cell surfaces. The complement system belongs to the innate immune system, and facilitates the elimination of viruses, bacteria, and other foreign invaders. Moreover, the complement system is involved in inflammation reactions and the blood clotting process. Therefore, complement activation has been widely examined in evaluating the biosafety of various biomaterials. Complement activation can be induced by three pathways (classic, alternative, and mannan-binding lectin pathways) involving multistep protein cleavage cascades. The enzyme, C3 convertase, is in common with all three pathways; it cleaves the complement component C3−C3a and C3b. Differing from labile C3b, C3a can exist in a stable form in plasma, at a concentration that indicates the degree of complement activation. In the present work, complement activation by the fluorescent carbon dots was assessed by detecting the C3a concentration.

Figure 7 demonstrates the concentration of C3a in the blood plasma after exposure to the fluorescent carbon dots. The C3a concentration in the presence of 0.1 or 1 mg/mL of the carbon dots was not significantly different from that of the negative control, while the C3a concentration in the presence of 5 mg/mL of the carbon dots was significantly higher than that of the negative control. These results indicate that 5 mg/mL of carbon dots significantly activates the complement system. The mechanisms of complement activation by biomaterials have been extensively investigated, though they are not yet completely understood. In any case, the physicochemical properties of biomaterial surfaces are known to determine the extent of complement activation. For instance, hydrophobic surfaces were reported to be more potent activators of the complement system than hydrophilic surfaces,[17] and the presence of chemical groups such as NH_2, OH, or COOH can affect complement activation.[18] From these clues, the hydroxyl and carboxyl groups and the hydrophobic structures of the fluorescent carbon dots are speculated to be complement activators. In light of previous reports, carbon nanotubes[19] and even PEGylated carbon nanotubes[20] may also activate the complement system.

3.6. Effect of Fluorescent Carbon Dots on in Vitro Blood Coagulation. Blood coagulation is one of the most important functions of blood tissue. Desirable blood coagulation should take place on particular occasions, such as during unexpected bleeding. Too weak or too strong blood coagulation ability could cause harmful or even lethal outcomes. Blood coagulation is achieved by the coagulation system, composed of three important components: clotting factors, fibrinogen, and platelets. The individual biofunctions of the

DOI: 10.1021/acsami.5b04866
ACS Appl. Mater. Interfaces 2015, 7, 19153−19162

components can be weakened or strengthened by the presence of agonists or activators, which can impair the normal blood clotting function. Biomaterials that contact blood tissue often act as agonists or activators of the coagulation system by interacting with the coagulation components, possibly causing adverse effects to the host. Hence, the effect of biomaterials on blood coagulation must be evaluated in preclinical tests.

3.6.1. APTT and PT. APTT and PT are routine examination parameters used for blood plasma coagulation in the clinic. The blood coagulation cascade contains three pathways: intrinsic, extrinsic, and common pathways.[21] APTT refers to the time required for a fibrin clot to form after the addition of a partial thromboplastin reagent and $CaCl_2$. It indicates the level of the intrinsic coagulation pathway. PT refers to the time required for a fibrin clot to form after the addition of tissue thromboplastin, indicating the level of the extrinsic coagulation pathway.[21] In this work, APTT and PT were measured to evaluate the effects of the fluorescent carbon dots on the intrinsic and extrinsic coagulation pathways, respectively.

Figure 8 shows the APTT and PT data for plasma containing the fluorescent carbon dots. From the statistical analysis, 0.1 mg/mL of the carbon dots did not significantly change the APTT or PT, compared to the PBS controls, while 1 and 2 mg/mL of the carbon dots caused significantly higher APTT and PT values, compared to the PBS controls. These results suggest that the fluorescent carbon dots at 0.1 mg/mL did not interfere with the intrinsic or extrinsic coagulation pathways, but at concentrations of 1 and 2 mg/mL, they exhibited anticoagulant properties. This may be explained by the interaction of the carbon dots with clotting factors and/or fibrinogen and possibly impairing their biofunctions.

3.6.2. TEG. The above APTT and PT assays reflect coagulation times for blood plasma. In contrast, TEG measures the overall, dynamic process of whole blood coagulation by detecting the blood clot strength. Hence, it provides more information on the activity of the clotting system. The TEG assay has four key parameters:[21] (1) reaction time (R), the time from adding the initiator $CaCl_2$ to the formation of the initial fibrin; (2) coagulation time (K), the dynamics of clot formation; (3) α angle, clot polymerization rate or the rapidity of fibrin cross-linking; and (4) maximum amplitude (MA) of the tracing, the maximum blood clot strength. Beyond the normal range provided by the TEG analyzer, a higher R value means lower activity of the clotting factors; higher K values, lower α values, or both mean lower activity of fibrinogen; and a lower MA value means lower activity of platelets, and vice verse. In virtue of its advantages, TEG has been widely used clinically and in blood-related research. In this work, TEG was used to better understand the effects of the fluorescent carbon dots on the whole blood clotting process.

Figure 9 shows TEG traces of the whole blood coagulation process in the presence of the carbon dots, with the corresponding parameters listed in Table 1. From Figure 9, the TEG traces in the presence of 0.1 and 1 mg/mL carbon dots were similar to the control, while the TEG trace in the presence of 5 mg/mL carbon dots appeared to be abnormal, compared to the control. From Table 1, the four TEG parameters in the presence of 0.1 mg/mL carbon dots were all in the normal range. In the presence of 1 mg/mL carbon dots, only α was slightly lower than the normal range, and the other three parameters were all in the normal range. In the presence of 5 mg/mL carbon dots, the four parameters were all beyond the normal range, suggesting that the carbon dots at 5 mg/mL impaired the activity of the clotting system. These results suggest that 1 mg/mL carbon dots in the whole blood could be a safe concentration for the blood clotting system.

3.7. Platelet Activation by Fluorescent Carbon Dots. Activation of resting platelets is a key step in the coagulation cascade. Platelets are sensitive to the presence of foreign biomaterials that can enhance or attenuate the activity of platelets and further affect the blood coagulation function. Therefore, the interaction between platelets and biomaterials is particularly important, and platelet activation is frequently measured in evaluations of biomaterials and blood compatibility. Activated platelets can be indicated by the expression of some biomarkers. For instance, platelet activation marker CD62P (P-Selectin) is overexpressed on the surface of activated platelets, with its concentration indicating the degree of platelet activation, and reflecting the risk of thrombus formation.

In this work, platelet activation by fluorescent carbon dots was measured by the P-Selectin expression on platelets in the presence of the carbon dots (Figure 10). The carbon dots, at 0.01 and 0.1 mg/mL, caused significantly higher platelet activation, compared to the negative control, while platelet activation in the presence of 1 mg/mL of the carbon dots was not significantly different from the negative control. This implies that the carbon dots have two-sided effects on platelets, as platelet activator and causing cytotoxicity. The former can be attributed to the presence of hydrophobic structures on the carbon dots, as hydrophobic structures have been reported to enhance platelet activation.[22,23] The latter may result from a disturbed platelet membrane structure caused by the carbon dots, as shown in the above results for RBC morphology and lysis. As a result, a low concentration of carbon dots with low cytotoxicity tends to activate platelets, whereas carbon dots at a high concentration are mainly cytotoxic to the structure and function of platelets.

3.8. Effect of Intravenously Administered Fluorescent Carbon Dots on Blood Coagulation. In vivo biocompatibility evaluation of carbon dots is important for directing their clinical application. Sun et al. reported an in vivo toxicity evaluation of intravenously injected carbon dots, and found that doses up to 40 mg/kg body weight did not cause detectable toxic effects on the structure or function of liver, kidney, and spleen.[6] To study the in vivo hemocompatibility of carbon dots, we measured the APTT and PT of blood collected from rats, 24 h after intravenously injecting them with the fluorescent carbon dots. Figure 11 shows that the APTT and PT data for the rats injected with carbon dots was not significantly different from the control. Thus, intravenous administration of carbon dots at doses up to 50 mg/kg seems to be safe for the blood coagulation function of rats.

The in vitro hemocompatibility and in vivo hemocompatibility evaluations reveal a great difference. The in vitro hemocompatibility evaluation was conducted in a closed system; however, for the in vivo evaluation, the circulatory system is not a closed lumen and the blood components can be exchanged with the extravascular system. When nanomaterials are administered into blood tissue, they are often instantly recognized and removed from the circulation by the mononuclear phagocyte system. Consequently, the concentration of materials in the blood will rapidly change over time. The in vitro hemocompatibility study helps to reveal the interactions and mechanisms existing between the materials and the blood components, while the in vivo hemocompatibility

DOI: 10.1021/acsami.5b04866
ACS Appl. Mater. Interfaces 2015, 7, 19153−19162

study provides more practical data for directing the clinical applications.

4. CONCLUSION

In this work, we investigated the effects of α-cyclodextrin-based fluorescent carbon dots on the structure and function of key blood components at cellular and molecular levels. We found that the carbon dots, at concentrations of ≤0.1 mg/mL, neither alter RBC morphology nor cause RBC lysis. With concentrations of carbon dots up to 0.2 mg/mL, the local microenvironment of fibrinogen was disturbed but only a weak effect was observed on the secondary structure of fibrinogen. Concentrations of carbon dots, up to 1 mg/mL, in blood plasma did not cause significant complement activation. The carbon dots at 0.1 mg/mL in blood plasma did not cause a significant change to the in vitro APTT and PT data, and 1 mg/mL of the carbon dots in whole blood did not cause an adverse impact to the in vitro whole blood coagulation. The carbon dots tend to be platelet activators only at low concentrations. Intravenous administration of the carbon dots, at doses up to 50 mg/kg, did not impair the blood coagulation function. These findings provide important information for circumventing the potential risks and for promoting the clinical applications of the fluorescent carbon dots.

■ ASSOCIATED CONTENT

Supporting Information

The Supporting Information is available free of charge on the ACS Publications website at DOI: 10.1021/acsami.5b04866.

Quantitative analysis for the cellular uptake of the carbon dots, morphology of the carbon dots-treated RBCs in the presence of BSA, lysis of the carbon dots-treated RBCs in the presence of BSA, in vitro APTT and PT data, and experimental details (PDF)

■ AUTHOR INFORMATION

Corresponding Author

*E-mail: tliuzonghua@jnu.edu.cn. Tel/Fax: 86-20-85226397.

Notes

The authors declare no competing financial interest.

■ ACKNOWLEDGMENTS

This work was financially supported by the National Natural Science Foundation of China (Grant No. 81101151) and the Science and Technology Project of Guangdong Province (2014A040401028).

■ REFERENCES

(1) Yang, Z. C.; Wang, M.; Yong, A. M.; Wong, S. Y.; Zhang, X. H.; Tan, H.; Chang, A. Y.; Li, X.; Wang, J. Intrinsically Fluorescent Carbon Dots with Tunable Emission Derived from Hydrothermal Treatment of Glucose in the Presence of Monopotassium Phosphate. *Chem. Commun.* **2011**, *47*, 11615−11617.

(2) Xu, X.; Ray, R.; Gu, Y.; Ploehn, H. J.; Gearheart, L.; Raker, K.; Scrivens, W. A. Electrophoretic Analysis and Purification of Fluorescent Single-Walled Carbon Nanotube Fragments. *J. Am. Chem. Soc.* **2004**, *126*, 12736−12737.

(3) Esteves Da Silva, J. C. G.; Goncalves, H. M. R. Analytical and Bioanalytical Applications of Carbon Dots. *TrAC, Trends Anal. Chem.* **2011**, *30*, 1327−1336.

(4) Baker, S. N.; Baker, G. A. Luminescent Carbon Nanodots: Emergent Nanolights. *Angew. Chem., Int. Ed.* **2010**, *49*, 6726−6744.

(5) Das, B.; Dadhich, P.; Pal, P.; Srivas, P. K.; Bankoti, K.; Dhara, S. Carbon Nanodots from Date Molasses: New Nanolights for the in vitro Scavenging of Reactive Oxygen Species. *J. Mater. Chem. B* **2014**, *2*, 6839−6847.

(6) Yang, S. T.; Wang, X.; Wang, H. F.; Lu, F. S.; Luo, P. J. G.; Cao, L.; Meziani, M. J.; Liu, J. H.; Liu, Y. F.; Chen, M.; Huang, Y. P.; Sun, Y. P. Carbon Dots as Nontoxic and High-Performance Fluorescence Imaging Agents. *J. Phys. Chem. C* **2009**, *113*, 18110−18114.

(7) Kainthan, R. K.; Gnanamani, M.; Ganguli, M.; Ghosh, T.; Brooks, D. E.; Maiti, S.; Kizhakkedathu, J. N. Blood Compatibility of Novel Water Soluble Hyperbranched Polyglycerol-based Multivalent Cationic Polymers and Their Interaction with DNA. *Biomaterials* **2006**, *27*, 5377−5390.

(8) Cayuela, A.; Soriano, M. L.; Carrion, M. C.; Valcarcel, M. Functionalized Carbon Dots as Sensors for Gold Nanoparticles in Spiked Samples: Formation of Nanohybrids. *Anal. Chim. Acta* **2014**, *820*, 133−138.

(9) Fan, R. J.; Sun, Q.; Zhang, L.; Zhang, Y.; Lu, A. H. Photoluminescent Carbon Dots Directly Derived from Polyethylene Glycol and Their Application for Cellular Imaging. *Carbon* **2014**, *71*, 87−93.

(10) Liu, Z. H.; Jiao, Y. P.; Wang, T.; Zhang, Y. M.; Xue, W. Interactions between Solubilized Polymer Molecules and Blood Components. *J. Controlled Release* **2012**, *160*, 14−24.

(11) Liu, Z. H.; Janzen, J.; Brooks, D. E. Adsorption of Amphiphilic Hyperbranched Polyglycerol Derivatives onto Human Red Blood Cells. *Biomaterials* **2010**, *31*, 3364−3373.

(12) Baba, T.; Rauch, C.; Xue, M.; Terada, N.; Fujii, Y.; Ueda, H.; Takayama, I.; Ohno, S.; Farge, E.; Sato, S. B. Clathrin-Dependent and Clathrin-Independent Endocytosis are Differentially Sensitive to Insertion of Poly (ethylene glycol)-Derivatized Cholesterol in the Plasma Membrane. *Traffic* **2001**, *2*, 501−512.

(13) Sevilla, M.; Fuertes, A. B. Chemical and Structural Properties of Carbonaceous Products Obtained by Hydrothermal Carbonization of Saccharides. *Chem. - Eur. J.* **2009**, *15*, 4195−4203.

(14) Sevilla, M.; Fuertes, A. B. The Production of Carbon Materials by Hydrothermal Carbonization of Cellulose. *Carbon* **2009**, *47*, 2281−2289.

(15) Lynch, I.; Dawson, K. A. Protein-Nanoparticle Interactions. *Nano Today* **2008**, *3*, 40−47.

(16) Venault, A.; Ballad, M. R. B.; Liu, Y. H.; Aimar, P.; Chang, Y. Hemocompatibility of PVDF/PS-b-PEGMA Membranes Prepared by LIPS Process. *J. Membr. Sci.* **2015**, *477*, 101−114.

(17) Thasneem, Y. M.; Sajeesh, S.; Sharma, C. P. Glucosylated Polymeric Nanoparticles: A Sweetened Approach against Blood Compatibility Paradox. *Colloids Surf., B* **2013**, *108*, 337−344.

(18) Ekdahl, K. N.; Nilsson, B.; Golander, C. G.; Elwing, H.; Lassen, B.; Nilsson, U. R. Complement Activation on Radio Frequency Plasma Modified Polystyrene Surfaces. *J. Colloid Interface Sci.* **1993**, *158*, 121−128.

(19) Salvador-Morales, C.; Flahaut, E.; Sim, E.; Sloan, J.; Green, M. L. H.; Sim, R. B. Complement Activation and Protein Adsorption by Carbon Nanotubes. *Mol. Immunol.* **2006**, *43*, 193−201.

(20) Hamad, I.; Hunter, A. C.; Rutt, K. J.; Liu, Z.; Dai, H.; Moghimi, S. M. Complement Activation by PEGylated Single-Walled Carbon Nanotubes is Independent of C1q and Alternative Pathway Turnover. *Mol. Immunol.* **2008**, *45*, 3797−3803.

(21) Zhong, D.; Jiao, Y. P.; Zhang, Y.; Zhang, W.; Li, N.; Zuo, Q. H.; Wang, Q.; Xue, W.; Liu, Z. H. Effects of the Gene Carrier Polyethyleneimines on Structure and Function of Blood Components. *Biomaterials* **2013**, *34*, 294−305.

(22) Leszczak, V.; Popat, K. C. Improved in vitro Blood Compatibility of Polycaprolactone Nanowire Surfaces. *ACS Appl. Mater. Interfaces* **2014**, *6*, 15913−15924.

(23) Jin, J.; Huang, F.; Hu, Y.; Jiang, W.; Ji, X.; Liang, H.; Yin, J. Immobilizing PEO-PPO-PEO Triblock Copolymers on Hydrophobic Surfaces and its Effect on Protein and Platelet: A Combined Study Using QCM-D and DPI. *Colloids Surf., B* **2014**, *123*, 892−899.

DOI: 10.1021/acsami.5b04866
ACS Appl. Mater. Interfaces 2015, 7, 19153−19162